RSC Advances

PAPER

View Article Online
View Journal | View Issue

Cite this: *RSC Adv.*, 2021, **11**, 18476

Robust, flexible, and high-performance electromagnetic interference shielding films with long-lasting service

Licui Wang,[a] Zhaoxin Xie,[a] Yanhu Zhan, *[ab] Xuehui Hao,[a] Yanyan Meng,[a] Shi Wei,[b] Zhenming Chen*[b] and Hesheng Xia *[c]

It is of great significance for electromagnetic interference (EMI) shielding materials to fulfill long-lasting service requirements. Here, waterborne polyurethane (WPU) was coated on the surface of a silver nanowire (AgNW) network with sputter-deposited nickel nanoparticles (NiNPs) by dip-coating technology to improve their durability. After five dip-coating cycles, a WPU layer nearly coated the whole surface of the hybrid papers, and only a fraction of the metal filler is bare. The resultant hybrid papers exhibit an electrical conductivity of ~3500 S m^{-1}, remnant magnetization of 0.03 emu g^{-1}, saturation magnetization of 0.10 emu g^{-1}, and coercivity of 256 Oe. On the one hand, the presence of the WPU coating does not affect the shielding effectiveness (SE) of the hybrid papers; on the other hand, the WPU coating enhances the ability to resist tape peeling. Moreover, the resultant hybrid papers still maintain the original SE value (~80 dB), even after exposure to air for 5 months owing to the isolation effect of the WPU coating, implying long-lasting durability. The results confirm that the obtained hybrid papers can meet the requirements of practical applications.

Received 8th April 2021
Accepted 11th May 2021

DOI: 10.1039/d1ra02756e

rsc.li/rsc-advances

Introduction

In recent times, electromagnetic interference (EMI) pollution has worsened worldwide owing to the rapid growth of wireless communication devices, especially the arrival of the 5G era.[1–3] To eliminate EMI pollution, the design and fabrication of high-performance EMI shielding materials are of great significance.[4,5] Compared with metal materials, conductive polymer composites (CPCs), consisting of polymers and conductive fillers, are the best candidates as EMI shielding materials because of their intrinsic properties, such as flexibility, easy processing, low cost, and anticorrosion.[6–8] It is well known that the EMI shielding effectiveness (SE) of CPCs is strongly contingent on the type and topology of conductive fillers.[9–13] Among conductive fillers, silver nanowires (AgNWs) are attractive to researchers because of their excellent electrical conductivity (6.3×10^7 S m^{-1}) and high aspect ratio, which is beneficial in constructing a conductive network at low concentration.[14,15] To improve the performance of AgNWs and obtain excellent CPC-based EMI shielding materials, a conductive network with interconnected AgNWs was formed on the surface of polymer films by spraying[16] and coating.[17] Lee *et al.* found that AgNW/cellulose papers fabricated by the dip-coating method exhibited an electrical conductivity of 6751 S m^{-1} and EMI SE of ~48.6 dB.[18]

According to Fresnel's equation, the EMI SE of CPCs is inseparable from their electrical conductivity and the magnetic permeability.[19] To enhance the electrical conductivity of the AgNW network on the surface of CPCs, subsequently improving their EMI SE, several methods, such as welding,[20] mechanical pressing,[21] and sintering,[22] have been developed. For example, Liang *et al.* demonstrated that the SE value of AgNW films increases from 5 dB to 25 dB *via* UV-induced welding.[23] Very recently, our groups reported a novel approach to simultaneously enhancing the magnetic and electrical conductivity of AgNW networks by magnetron sputtering technology, which is an efficient method to form metal films on a substrate.[24] The SE of AgNW/cellulose paper with sputter-deposited nickel nanoparticles (NiNPs) is 1.13 times higher than that of the system without NiNPs because NiNPs endow hybrid films with superior electrical conductivity and magnetic properties.

Of note, it is of paramount importance to extend the service life of CPC-based EMI shielding materials under external mechanical deformations or air. Nevertheless, AgNWs and NiNPs were easily peeled from the polymer films because of weak adhesion. More importantly, bare AgNWs and NiNPs can unavoidably be oxidized or even corroded in the atmosphere. The above two cases result in degraded electrical conductivity and EMI SE for CPCs.[22,25,26] Coating with polymers is an effective

[a]*School of Materials Science and Engineering, Liaocheng University, Liaocheng, 252000, China. E-mail: zhanyanhu@lcu.edu.cn; zhanyanhu@163.com*
[b]*Guangxi Key Laboratory of Calcium Carbonate Resources Comprehensive Utilization, Hezhou University, Hezhou City, 542899, China. E-mail: chenzhenming2@163.com*
[c]*State Key Laboratory of Polymer Materials Engineering, Polymer Research Institute, Sichuan University, Chengdu 610065, China. E-mail: xiahs@scu.edu.cn*

approach to address these two issues. For example, under the aegis of a polyurethane (PU) layer, no obvious EMI SE degradation was observed for AgNW/carbon fibre fabric after ultrasonic treatment or tape peeling.[25] EMI SE of MXene/AgNW film was still 34.8 dB after peeling off cycles because AgNWs were partly embedded into a poly(vinyl alcohol) film.[27] In our previous paper, 1*H*,1*H*,2*H*,2*H*-perfluorodecanethiol was employed to enhance the hydrophobicity of AgNW/cellulose papers with sputter-deposited NiNPs, but the resultant papers have a poor ability to resist tape peeling.[24]

Herein, robust, flexible, and high-performance EMI shielding films with long-lasting service were fabricated *via* a simple approach. NiNPs were first deposited on the surface of AgNW-coated cellulose filter paper by a magnetron sputter procedure, and then waterborne polyurethane was coated on the above film. To evaluate stable shielding performance, we measured the SE of the resultant films, which underwent a vigorous external environment, *e.g.*, blending, peeling, and a strong alkali solution. The films were first exposed to air for 5 months, and then their SE is tested to assess their long-lasting service.

Experimental

Materials

Cellulose filter papers with a diameter of 7 cm (CFP, 0.42 g cm^{-3}), hydrochloric acid (HCl), sodium hydroxide (NaOH), and sodium chloride (NaCl) were supplied by Sinopharm Chemical Reagent Co., Ltd. (China). Waterborne polyurethane solution (WPU, 40 wt%, AMS-2066) was supplied by Guangzhou Yumay Chemical Co., Ltd. (China). Silver nanowire solution with a concentration of 20 mg mL^{-1} (XFJ03, diameter: 50 ± 5 nm, length: 100–200 μm) was obtained from Nanjing XFNANO Materials Tech Co., Ltd. (China). A nickel target with a purity of 99.995% was purchased from ZhongNuo Advanced Material (Beijing) Technology Co., Ltd. (China).

Fabrication of CFP/AgNW/NiNP/WPU hybrid papers

CFP/AgNW/NiNP (CSN) papers were fabricated according to our previous paper.[24] In brief, AgNWs were covered on CFP with ~0.2 mm thickness by dip-coating over 20 cycles. Subsequently, NiNPs were deposited on one surface of CFP/AgNW paper for 15 min by a magnetron sputtering apparatus to obtain the CSN papers with a diameter of 7 cm. The DC power, temperature, base, and working pressure were 50 W, 28 °C, 5.0×10^{-4} Pa, and 0.5 Pa, respectively, during the magnetron sputtering procedure.

The resulting papers were dipped into 10 wt% WPU solution, which was obtained by diluting the original solution, for 3 s and then dried at 60 °C for 15 min. The above process was repeated until the desired cycles. The obtained hybrid papers were named $CSNPU_x$, where x means the dip-coating cycles in WPU solution.

Characterization

A Zeiss Ultra 55 apparatus (Jena, Germany) was used to observe the morphology of CSNPU papers at an accelerating voltage of 3 kV. All specimens were sputter-coated with gold before SEM observation. X-ray energy dispersion spectroscopy (EDS, Oxford Instruments, coupled to SEM microscopy) was used to analyse the chemical composition of the CSNPU papers by applying a 9 kV acceleration voltage under an 8.5 mm working distance. A diffractometer (D8 Advanced, Bruker Co., Germany) was employed to record the X-ray diffraction (XRD) patterns of the CSNPU papers. The spectra were recorded in transmission mode with 2θ values ranging from 5° to 60° at 40 kV. A picometer (Keithley 2000) system was used to measure the electrical conductivity of the resultant papers. Magnetic properties were studied using a vibratory sample magnetometer (PPMS-9, Quantum Design, USA) at room temperature with an applied field of −10 000 to 10 000 Oe. A vector network analyzer (Agilent N5247A) was employed to analyse the EMI SE of the resultant papers in the X-band (8.2–12.4 GHz). The diameter and thickness of the measured samples were 13 mm and ~0.2 mm, respectively.

Results and discussion

XRD analysis of CSNPU papers

Fig. 1 displays XRD patterns of $CSNPU_0$ and $CSNPU_5$ papers. It is evident that no obvious discrepancy in the XRD patterns is observed before and after coating the WPU layers. All hybrid papers show the same characteristic diffraction peaks. The same diffraction peaks were located at $2\theta = 38.2°$, 44.4°, 64.5°, and 77.5°, assigned to the (111), (200), (220), and (311) fcc crystal planes of AgNWs, respectively, where the characteristic peaks at $2\theta = 14.9°$, 16.4° and 22.6° were attributed to the $(1\bar{1}0)$, (110), and (200) planes of cellulose, respectively.[28–30] Evidently, compared with the Ag (200) peak, the intensity of the Ag (111) peak is high, implying a polycrystalline structure with a strong Ag (111) preferred orientation, benefiting the construction of a perfect conductive network at a low concentration and enhancing the EMI SE of CPCs. It is hard to ignore that for all samples, the (111) peak of NiNPs at $2\theta = 44.6°$ is so weak that it is covered by the strong peak of (200) of AgNWs at $2\theta = 44.5°$

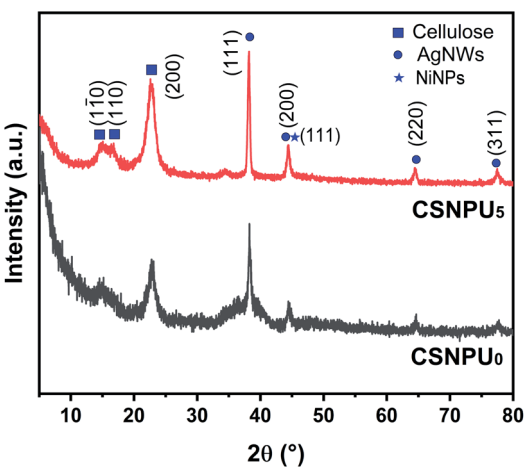

Fig. 1 XRD patterns of $CSNPU_0$ and $CSNPU_5$ papers.

because the NiNP content is extremely low, as it was in our previous report.[24] SEM images and EDS spectra of CSNPU papers are used to support the attendance of NiNPs in the next section.

Morphology of CSNPU papers

The microstructure of CPCs strongly affects their properties,[31] so the resulting CSNPU paper morphology was observed by SEM and is displayed in Fig. 2. It is easy to find the interconnected AgNW network at low magnification (Fig. 2a and a′). For the image with high magnification (Fig. 2a″), the surface of AgNWs is no longer smooth and covered uniformly by some granulum, *i.e.*, NiNPs, after the magnetron sputtering process. For $CSNPU_1$ papers, some surfaces were coated by WPU (the region surrounded by red dots in Fig. 2b′), but most metal fillers were exposed (Fig. 2b and b′). At high magnification (Fig. 2b″), the WPU layer embraces AgNWs with sputter-deposited NiNPs. In the case of $CSNPU_5$ papers, WPU nearly coated the whole surface, and very few metal fillers were bare (Fig. 2c, c′ and c″). The WPU layers, as protective clothing, enable the materials to resist vigorous external environments. Unfortunately, some microcracks can be found (Fig. 2c″). Subsequently, EDS analysis was employed to further investigate the distribution of AgNWs and NiNPs. SEM images with elemental mapping and EDS spectra of $CSNPU_0$ and $CSNPU_5$ papers are summarized in Fig. 3. Elemental mappings for $CSNPU_0$ papers, as shown in Fig. 3a, demonstrate that NiNPs are deposited on the surface of AgNWs and form a compact layer, which is helpful for enhancing the electrical conductivity of the AgNW conductive network. Notably, the uniform WPU coating does not affect the distribution of AgNWs and NiNPs, as shown in Fig. 3b. As expected, compared with $CSNPU_0$ papers, the resultant $CSNPU_5$

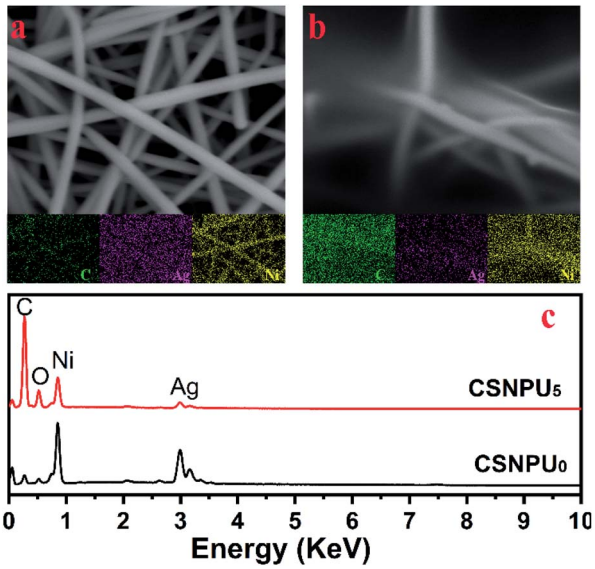

Fig. 3 SEM image with elemental mappings of $CSNPU_0$ (a), and $CSNPU_5$ (b) papers; EDS spectra of $CSNPU_0$, and $CSNPU_5$ papers (c).

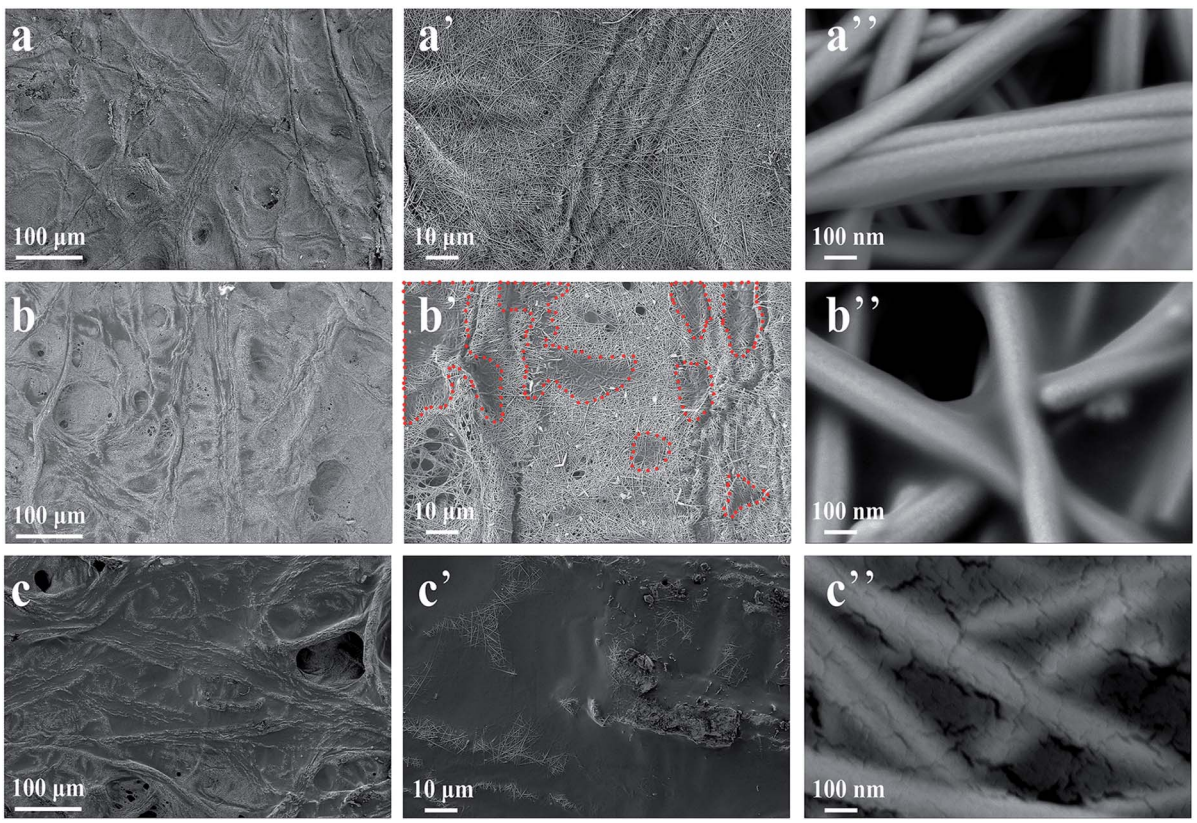

Fig. 2 SEM images of $CSNPU_0$ papers (a, a′ and a″), $CSNPU_1$ papers (b, b′ and b″) and $CSNPU_5$ papers (c, c′ and c″).

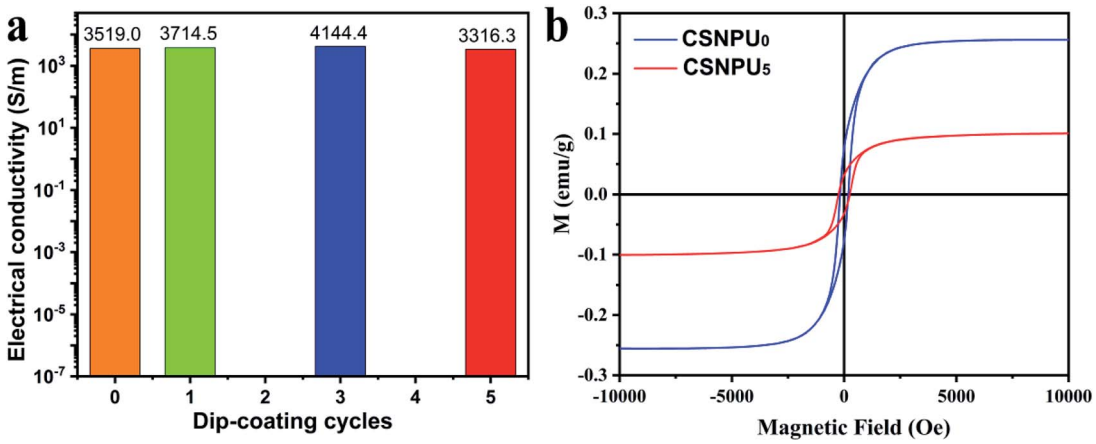

Fig. 4 Electrical conductivity (a) and hysteresis loop (b) of CSNPU papers.

papers exhibit the C peak with remarkably strong intensity, confirming the presence of the WPU coating (Fig. 3c).

Electrical conductivity and magnetic properties of CSNPU papers

In general, excellent electrical conductivity, coupled with magnetic properties, would capacitate CPCs to exhibit outstanding EMI SE.[19] The effect of the deposited mass of NiNPs on their electrical conductivity and magnetic properties was discussed in detail in a previous report.[24] Here, we only research the effect of the WPU coating on the electrical conductivity and magnetic properties of CSNPU papers, as displayed in Fig. 4. Fig. 4a displays that the electrical conductivity of $CSNPU_0$ papers reaches 3519.0 S m^{-1} and that the electrical conductivity of CSNPU papers is similar with that of $CSNPU_0$ paper when the number of dip-coatings increases from 1 to 5, implying that the conductive network is too stable to be broken. Fig. 4b shows the typical S-shaped hysteresis loop for CSNPU papers. $CSNPU_5$ papers have a remnant magnetization (M_r) of 0.03 emu g^{-1} and saturation magnetization (M_s) of 0.10 emu g^{-1}, which are lower than those of $CSNPU_0$ papers (M_r: 0.08 emu g^{-1}; M_s: 0.26 emu g^{-1}) and attributed to the attendance of a nonmagnetic WPU coating. In addition, the coercivity (H_c) of $CSNPU_0$ and $CSNPU_5$ papers are 182 Oe and 256 Oe, respectively.

EMI SE of CSNPU papers

Fig. 5a presents the EMI SE of CSNPU papers in X-band at room temperature. It is worth noting that the EMI SEs of all CSNPU papers are independent of the frequency. Ultrahigh electrical conductivity, as well as good magnetic properties, endows $CSNPU_0$ papers with excellent EMI SE (80.7 dB), better than that of the reported AgNW/poly(diallyldimethyl-ammonium chloride) films (31.3 dB).[32] Remarkably, a nonobvious change in the SE value was found after dip-coating the WPU layer, as shown Fig. 5a. This is attributed to the AgNW network with sputter-deposited NiNPs being impregnable during the dip-coating process. In general, the EMI SE of CPCs is attributed to reflection mechanisms and absorption mechanisms. Reflection shielding (SE_R) and absorption shielding (SE_A) are calculated by S parameters, and the total EMI SE (SE_T) is equal to the sum of SE_R and SE_A.[19] Fig. 5b displays that for all CSNPU papers, the SE_A value is higher than the SE_R. For example, SE_T and SE_A of $CSNPU_5$ papers are 79.3 dB and 72.3 dB, respectively, while SE_R is only 7.0 dB. Compared with the reported Ag/polymer film (SE_T: 77.6 dB, SE_R: 13 dB),[33] $CSNPU_5$ papers exhibit a higher SE_T value and lower SE_R value, which is favor to decrease second pollution of EM wave. To investigate the shielding mechanisms, the power coefficients of transmissivity (T), absorption (A), and reflection (R) were calculated and are shown in Fig. 5c. For all

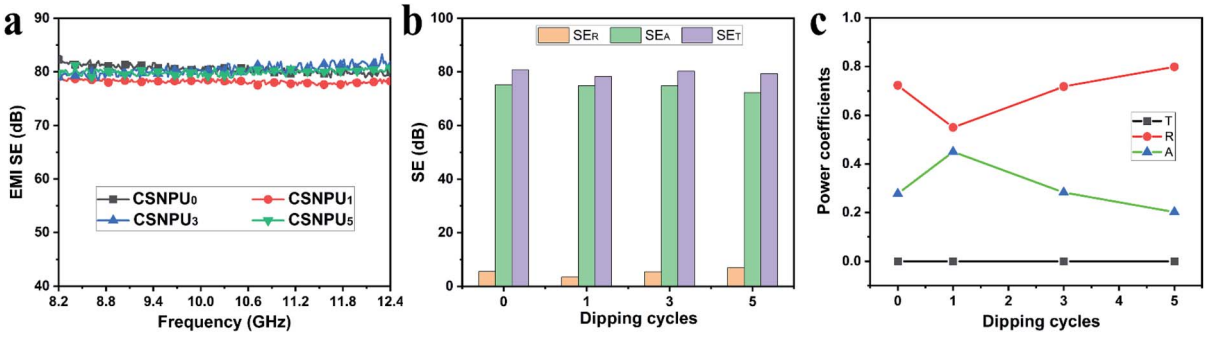

Fig. 5 EMI SE of CSNPU papers in X-band (a); SE_R, SE_A and SE_T of CSNPU papers at a frequency of 10.3 GHz (b); power coefficients of reflection, absorption and transmittance for the CSNPU papers as a function of dip-coating cycles (c).

CSNPU papers, the value of R is higher than that of A, which results from the impedance mismatch between air and hybrid papers. The result confirms that most of the initial power is reflected at the surface of the hybrid papers. From the EM energy point of view, therefore, the shielding mechanism of hybrid papers is reflection.[27] In addition, it is interesting to note that SE_A is greater than SE_R even for samples with high electrical conductivity and large reflectivity. The result can be explained by two reasons. The first is that SE_R is proportional to the logarithm of σ/μ (where σ and μ are the electrical conductivity and the magnetic permeability of shielding materials, respectively) according to Fresnel's equation.[34] The presence of NiNPs not only enhances the electrical conductivity of hybrid papers but also improves their magnetic permeability. The increasing magnetic permeability partially drained the contribution of the increased electrical conductivity to the SE_R. The second is that SE_A and SE_R were calculated by $SE_A = -10\lg\left(\frac{T}{1-R}\right) = -10\lg\left(\frac{T}{A+T}\right)$ and $SE_R = -10\lg(1-R) = -10\lg(A+T)$, respectively. The EM waves transmit through high electrically conductive shielding materials, so $T/(A+T)$ is far less than $(A+T)$, leading to SE_A being higher than SE_R, and similar results were also reported by Kwon *et al.*[35] For example, as shown in Fig. 5c, when an EM wave meets $CSNPU_5$ papers, 79.8306825% of the incident power is first reflected (SE_R of 7.0 dB), 20.1693164% is absorbed (SE_A of 72.3 dB), and only 0.0000011% can be transmitted.

Durability of CSNPU based EMI papers

Satisfactory performance stability is a critical factor for evaluating the application value of CPC-based EMI shielding

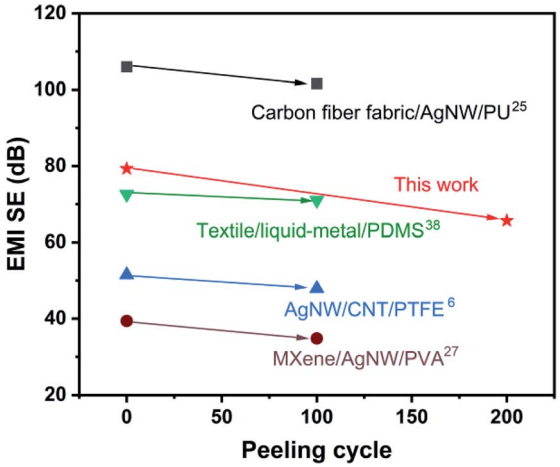

Fig. 7 Comparison of SE of the resultant papers and the reported papers before and after peeling test.

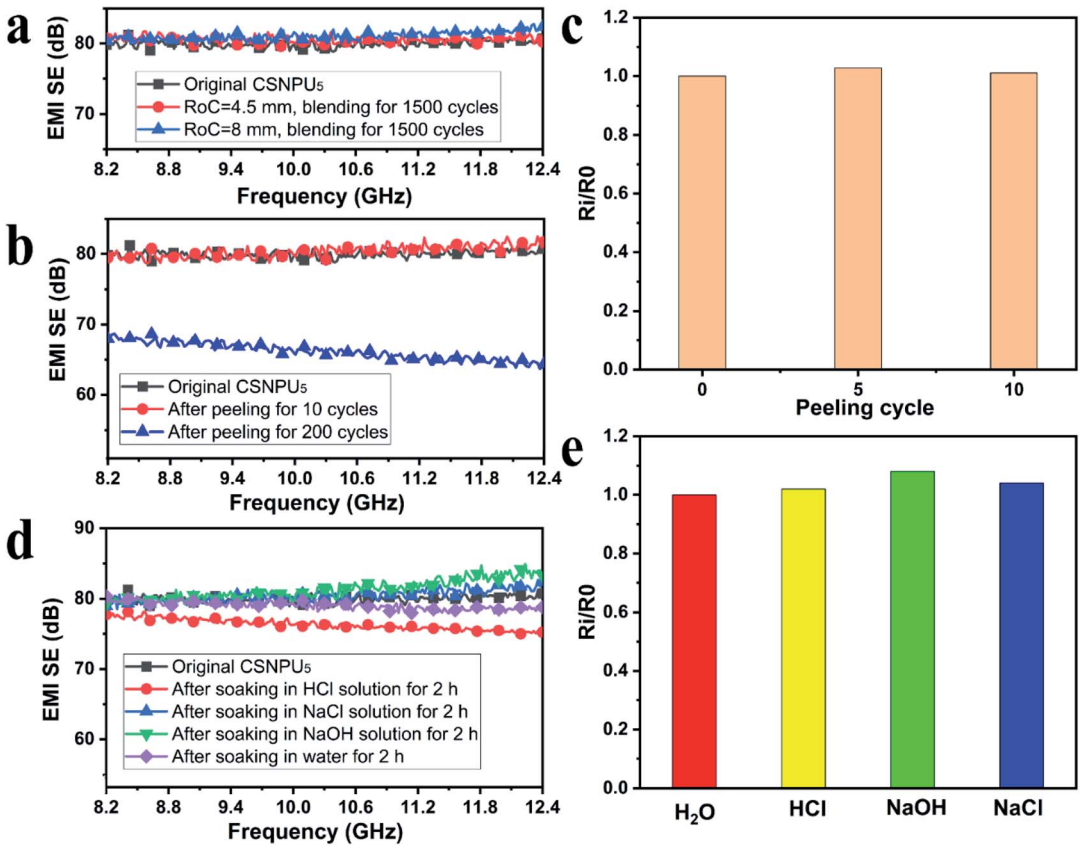

Fig. 6 SE value of $CSNPU_5$ paper after 1500 bending cycles at different radius of curvature (a); SE value (b) and the change of electrical conductivity (c) for $CSNPU_5$ paper after tape-peeling; EMI SE (d) and the change of electrical conductivity (e) for $CSNPU_5$ papers before and after immersing in different solvents (water, HCl solution, NaOH solution and NaCl solution) for 2 h.

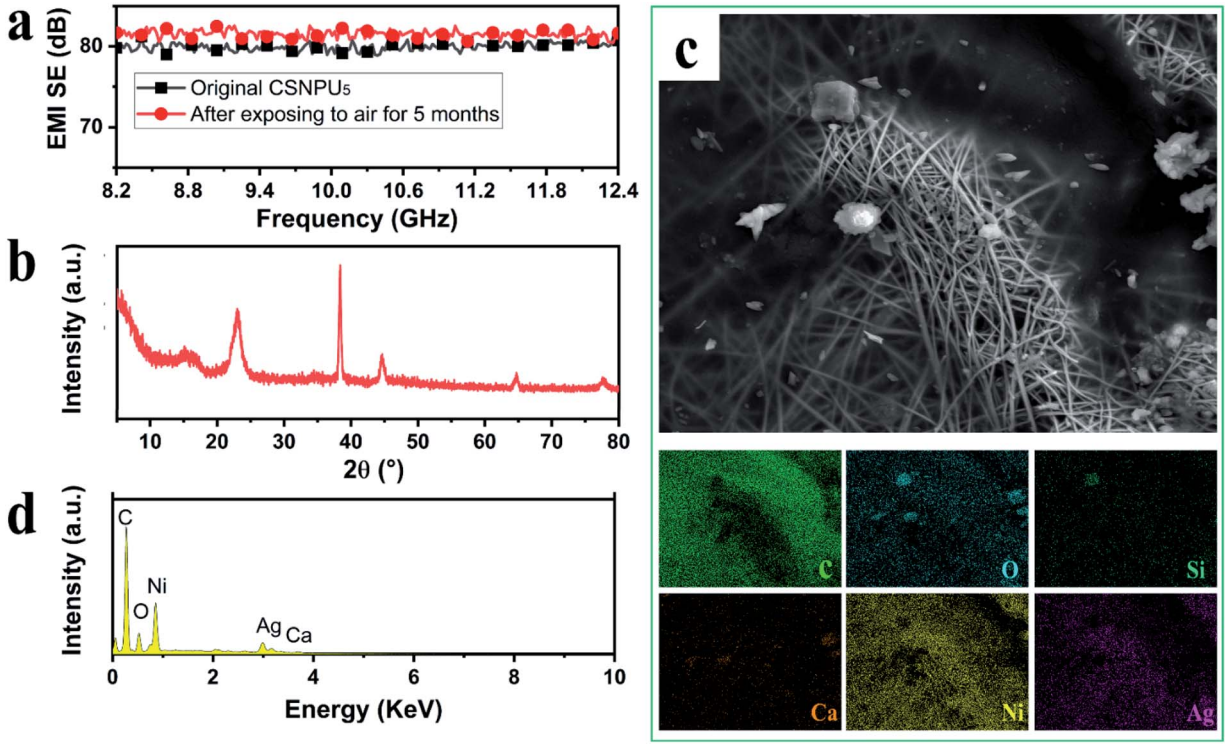

Fig. 8 SE value (a), XRD pattern (b), SEM image with elemental mapping (c) and EDS spectra (d) of $CSNPU_5$ paper after exposing to air for 5 months.

materials under harsh external environments, *e.g.*, mechanical deformation, strong alkali and acid solutions, peeling off and long exposure to air.[25,36–38] The bending stability of $CSNPU_5$ paper was tested and is shown in Fig. 6a. Compared with the original samples, the $CSNPU_5$ paper maintains a stable SE value after 1500 bending cycles at radii of curvature (RoCs) of 4.5 mm and 8 mm, indicating that the $CSNPU_5$ paper is robust enough to resist blending deformation. Fig. 6b displays that the EMI SE of $CSNPU_5$ paper remained at a high level of 80.6 dB after 10 tape-peeling cycles, attributable to the strong protection of WPU layers, leading to stable electrical conductivity (Fig. 6c). After 200 tape-peeling cycles, their SE decreases to 65.6 dB, which is still higher than that of the reported papers after the 100 peeling-cycles (Fig. 7) and far higher than the requirement of commercial EMI shielding materials (20 dB). Moreover, when immersed in NaOH solution (1 mol L^{-1}), NaCl solution (1 mol L^{-1}) and water for 2 h, $CSNPU_5$ papers still show an EMI SE similar to that of the original sample (Fig. 6d), ascribed to these solutions not harming the perfect conductive network (Fig. 6e). However, after soaking HCl solution (1 mol L^{-1}) for 2 h, the SE value of $CSNPU_5$ papers slightly decreased, ascribed to NiNPs being dissolved by HCl.[24] $CSNPU_5$ papers were exposed to air for 5 months to assess their long-lasting durability. As shown in Fig. 8a, after 5 months, the SE value of $CSNPU_5$ papers is ~80 dB, implying long-lasting service. This is attributed to the fact that the AgNWs and NiNPs cannot be oxidized owing to the isolation effect of the WPU layer (Fig. 8b). Fig. 8c shows an SEM image of $CSNPU_5$ paper that was exposed to air for 5 months. Except for the fact that some dust (the granule in Fig. 8c) adheres to the surface of the sample, its morphology is similar to that of the original samples (Fig. 2). Elemental mappings and EDS spectra of the exposed $CSNPU_5$ paper further demonstrate that no obvious change in the chemical element is found, as shown in Fig. 8c and d. Elemental Si and Ca are attributed to the dust.

Conclusions

In summary, we fabricated robust, flexible, and high-performance electromagnetic interference shielding films and investigated their morphology, electrical conductivity, magnetic properties, and durability in EMI shielding performance. Owing to the high electrical conductivity (~3500 S m^{-1}), the main shielding mechanism of CSNPU paper is a reflection mechanism. The WPU coatings could endure EMI shielding materials with high tolerance to harsh environments such as blending, tape peeling, and strong alkaline environments. Even after exposure to air for 5 months, the EMI SE of $CSNPU_5$ papers remained consistent with the initial value (~80 dB). These results confirm that the resultant CSNPU papers can meet the long-term service requirements of practical applications.

Conflicts of interest

There are no conflicts to declare.

Acknowledgements

This work was supported by the Natural Science Foundation of Shandong Province [ZR2019QEM009 and ZR2020QE026],

International Cooperative Research Program between the National Natural Science Foundation of China and the Italian Ministry of Foreign Affairs [5171101504], and the Natural Science Foundation of Guangxi [2018GXNSFAA281218, 2020GXNSFBA297139].

Notes and references

1 Y. Zhan, Y. Cheng, N. Yan, Y. Li, Y. Meng, C. Zhang, Z. Chen and H. Xia, *Chem. Eng. J.*, 2021, **417**, 129339.
2 Y. Wang, K. Ren, J. Sun, W. Li, S. Zhao, Z. Chen and J. Guan, *Compos. Sci. Technol.*, 2017, **140**, 89–98.
3 Y. Zhan, E. Lago, C. Santillo, A. E. Del Río Castillo, S. Hao, G. G. Buonocore, Z. Chen, H. Xia, M. Lavorgna and F. Bonaccorso, *Nanoscale*, 2020, **12**, 7782–7791.
4 Y. Chen, L. Pang, Y. Li, H. Luo, G. Duan, C. Mei, W. Xu, W. Zhou, K. Liu and S. Jiang, *Composites, Part A*, 2020, **135**, 105960.
5 E. Kim, D. Y. Lim, Y. Kang and E. Yoo, *RSC Adv.*, 2016, **6**, 52250–52254.
6 L.-C. Jia, G. Zhang, L. Xu, W.-J. Sun, G.-J. Zhong, J. Lei, D.-X. Yan and Z.-M. Li, *ACS Appl. Mater. Interfaces*, 2019, **11**, 1680–1688.
7 Y. Chen, L. Pang, Y. Li, H. Luo, G. Duan, C. Mei, W. Xu, W. Zhou, K. Liu and S. Jiang, *Composites, Part A*, 2020, **135**, 105960.
8 F. Liu, Y. Li, S. Hao, Y. Cheng, Y. Zhan, C. Zhang, Y. Meng, Q. Xie and H. Xia, *Carbohydr. Polym.*, 2020, **243**, 116467.
9 L.-C. Jia, D.-X. Yan, Y. Yang, D. Zhou, C.-H. Cui, E. Bianco, J. Lou, R. Vajtai, B. Li, P. M. Ajayan and Z.-M. Li, *Adv. Mater. Technol.*, 2017, **2**, 1700078.
10 X. Jin, J. Wang, L. Dai, X. Liu, L. Li, Y. Yang, Y. Cao, W. Wang, H. Wu and S. Guo, *Chem. Eng. J.*, 2020, **380**, 122475.
11 C. Song, X. Meng, H. Chen, Z. Liu, Q. Zhan, Y. Sun, W. Lu and Y. Dai, *Compos. Commun.*, 2021, 100632.
12 Y. Zhan, M. Oliviero, J. Wang, A. Sorrentino, G. G. Buonocore, L. Sorrentino, M. Lavorgna, H. Xia and S. Iannace, *Nanoscale*, 2019, **11**, 1011–1020.
13 Y. Zhan, Y. Meng and Q. Xie, *J. Appl. Polym. Sci.*, 2021, **107995**, 50597.
14 Y. Wang, F.-Q. Gu, L.-J. Ni, K. Liang, K. Marcus, S.-L. Liu, F. Yang, J.-J. Chen and Z.-S. Feng, *Nanoscale*, 2017, **9**, 18318–18325.
15 W. H. Sun, D. S. Hung, T. T. Song and S. F. Lee, *Ferroelectrics*, 2012, **435**, 148–154.
16 X. Zhang, Y. Zhong and Y. Yan, *Phys. Status Solidi A*, 2018, **215**, 1800014.
17 L.-C. Jia, D.-X. Yan, X. Liu, R. Ma, H.-Y. Wu and Z.-M. Li, *ACS Appl. Mater. Interfaces*, 2018, **10**, 11941–11949.
18 T.-W. Lee, S.-E. Lee and Y. G. Jeong, *ACS Appl. Mater. Interfaces*, 2016, **8**, 13123–13132.
19 Y. Zhan, J. Wang, K. Zhang, Y. Li, Y. Meng, N. Yan, W. Wei, F. Peng and H. Xia, *Chem. Eng. J.*, 2018, **344**, 184–193.
20 X. Liang, T. Zhao, W. Jiang, X. Yu, Y. Hu, P. Zhu, H. Zheng, R. Sun and C.-P. Wong, *Nano Energy*, 2019, **59**, 508–516.
21 L. Hu, H. S. Kim, J.-Y. Lee, P. Peumans and Y. Cui, *ACS Nano*, 2010, **4**, 2955–2963.
22 D. G. Kim, J. H. Choi, D.-K. Choi and S. W. Kim, *ACS Appl. Mater. Interfaces*, 2018, **10**, 29730–29740.
23 X. Liang, J. Lu, T. Zhao, X. Yu, Q. Jiang, Y. Hu, P. Zhu, R. Sun and C.-P. Wong, *Adv. Mater. Interfaces*, 2018, **353**, 1801635.
24 Y. Zhan, X. Hao, L. Wang, X. Jiang, Y. Cheng, C. Wang, Y. Meng, H. Xia and Z. Chen, *ACS Appl. Mater. Interfaces*, 2021, **13**, 14623–14633.
25 L.-C. Jia, L. Xu, F. Ren, P.-G. Ren, D.-X. Yan and Z.-M. Li, *Carbon*, 2019, **144**, 101–108.
26 J.-H. Pu, X.-J. Zha, L.-S. Tang, L. Bai, R.-Y. Bao, Z.-Y. Liu, M.-B. Yang and W. Yang, *ACS Appl. Mater. Interfaces*, 2018, **10**, 40880–40889.
27 B. Zhou, M. Su, D. Yang, G. Han, Y. Feng, B. Wang, J. Ma, J. Ma, C. Liu and C. Shen, *ACS Appl. Mater. Interfaces*, 2020, **12**, 40859–40869.
28 Z. Ma, S. Kang, J. Ma, L. Shao, Y. Zhang, C. Liu, A. Wei, X. Xiang, L. Wei and J. Gu, *ACS Nano*, 2020, **14**, 8368–8382.
29 R. Ou, Y. Xie, X. Shen, F. Yuan, H. Wang and Q. Wang, *J. Mater. Sci.*, 2012, **47**, 5978–5986.
30 Y. Zhan, Y. Meng, W. Li, Z. Chen, N. Yan, Y. Li and M. Teng, *Ind. Crops Prod.*, 2018, **122**, 422–429.
31 Y. Zhan, S. Hao, Y. Li, C. Santillo, C. Zhang, L. Sorrentino, M. Lavorgna, H. Xia and Z. Chen, *Compos. Sci. Technol.*, 2021, **205**, 108689.
32 X. Zhu, J. Xu, F. Qin, Z. Yan, A. Guo and C. Kan, *Nanoscale*, 2020, **12**, 14589–14597.
33 Z. Zeng, F. Jiang, Y. Yue, D. Han, L. Lin, S. Zhao, Y.-B. Zhao, Z. Pan, C. Li, G. Nyström and J. Wang, *Adv. Mater.*, 2020, **32**, 1908496.
34 Y.-J. Wan, X.-Y. Wang, X.-M. Li, S.-Y. Liao, Z.-Q. Lin, Y.-G. Hu, T. Zhao, X.-L. Zeng, C.-H. Li, S.-H. Yu, P.-L. Zhu, R. Sun and C.-P. Wong, *ACS Nano*, 2020, **14**, 14134–14145.
35 S. Kwon, R. Ma, U. Kim, H. R. Choi and S. Baik, *Carbon*, 2014, **68**, 118–124.
36 L.-X. Liu, W. Chen, H.-B. Zhang, Q.-W. Wang, F. Guan and Z.-Z. Yu, *Adv. Funct. Mater.*, 2019, **29**, 1905197.
37 Y. Zhou, Z. Sun, L. Jiang, S. Chen, J. Ma and F. Zhou, *Appl. Surf. Sci.*, 2020, **533**, 147431.
38 L.-C. Jia, X.-X. Jia, W.-J. Sun, Y.-P. Zhang, L. Xu, D.-X. Yan, H.-J. Su and Z.-M. Li, *ACS Appl. Mater. Interfaces*, 2020, **12**, 53230–53238.